Micro/Nanoscale Well and Channel Fabrication on Organic Polymer Substrates via a Combination of Photochemical and Alkaline Hydrolysis Etchings

Peng Yang,[†] Xu Zhang,[‡] Jingyi Xie,[†] Jinchun Chen,[‡] and Wantai Yang*,[†]

State Key Laboratory of Chemical Resource Engineering, Beijing, 100029, China, and Department of Polymer Science, Post Office Box 37, and College of Life Science and Technology, Beijing University of Chemical Technology, Beijing, 100029, China

Received June 5, 2006; Revised Manuscript Received August 11, 2006

With the utilization of photomasks, micro/nanoscale wells and channels with depths ranging from nanometers to several micrometers were fabricated on a poly(ethylene terephthalate) (PET) surface by a simple combination of photochemical and alkaline hydrolysis etching. The PET surface region could be directly and photochemically etched by UV light and *N*,*N*-dimethylformamide (DMF) to create 125−350 nm etching depths (step 1). In step 2, the depth could be further enlarged to 250−1400 nm by potassium hydroxide (KOH) developing. More importantly, when this combination etching was repeated with the same photomask, the depth increased with increasing etching times. For instance, the depth reached approximately 6 μm after a series of three combination etchings. The cross-sectional shape of the final structure was trapezoidal with smooth corners. No obvious widening effect in lateral size was observed after one combination etching, whereas the top width of the microfabricated channels was enlarged from 50 μm (the designed feature of the photomask used) to 100 μm after two or three combination etchings. Even more interesting was that step 1 resulted in the formation of a kind of aminated surface in the channel (6.5% amine content), but when step 2 was conducted, the aminated surface was erased. This process could be reversibly carried out by repeating step 1 (amination) and step 2 (erasing). Electrostatical self-assembly of an antibody, fluorescein isothiocyanate-labeled immunoglobulin G (FITC−IgG, goat anti-rabbit), was achieved on the aminated surface of the etched channels, which demonstrated that by this combination strategy, micro/nanoscale channels or wells featuring tunable depths and functional channel surfaces could be readily fabricated. Undoubtedly, these functionalized channels or wells onto organic substrates could provide a potential platform for microchips toward various functions such as microarrays, heterogeneous immunoassays, biosensors, concentrations, filtrations, and microanalysis.

Introduction

The fabrication of micro/nanostructures on material surfaces plays a fundamental role with increasing importance for advanced technologies including well-developed microelectronics and some emerging fields such as micro/nanoarrays of proteins,[1] micro/nanofluidics,[2] and microreactors.[3] The latter would bring revolutionary changes in traditional biomedicine,[4] analytical techniques,[5] and chemical engineering,[6] if the fabrication cost and prototyping time could be significantly decreased in order to achieve large-scale applications of the products.[7] Accordingly, more and more effort is put into developing relatively simple and low-cost fabrication techniques on organic polymer surfaces, replacing expensive photolithography on inorganic silicon.[7b] Micro/nanostructures could provide high or low aspect ratios for different applications. High aspect ratios offer the possibility of a higher packing density of microstructural elements and a higher throughput in continuous flow systems.[8] In contrast, shallow profiled structures with low aspect ratios, that is, depths from several micrometers down to nanometers, are desirable and necessary in single or integrated microfluidic chips for filtration, separation, concentration, or sorting functions[9] and nanochannels for single DNA analysis,[10] as well as microwells for protein microarrays.[11] When a microwell is used as a platform for a protein microarray, its depth has to be minimized to allow a free diffusion of analyte in the microwell.[11] Up until now, typical fabrication techniques for shallow micro/nanostructures mainly rely on molding,[12] templating,[13] lithography,[14,15] nanoembossing,[16] nanoimprinting,[17] self-assembly of copolymers,[18] stretching,[19] and lipid membrane technology.[20] As an example, Yu and Ober[15] combined photolithography and soft lithography to fabricate hybrid hydrogel microstructures for protein microarrays, where grooves with depths of ∼3 μm were obtained on the hydrogel surface by an imprinting or molding process from a stamp.

Poly(ethylene terephthalate) (PET), a polymer substrate stable against the exposure of aggressive solvents or high temperatures, has been widely used in microchip fabrication.[7b] Very recently, we reported on a new photochemical reaction between *N*,*N*-dimethylformamide (DMF) and a PET substrate under UV irradiation, which initiated an aminolysis[21] or photograft polymerization on the surface.[22] In the previous study,[21] we mainly reported on three points: (1) a detailed description of a new photochemical reaction called "UV-induced surface aminolysis reaction" (USAR) on a PET surface; (2) the use of USAR and a photomask to prepare a patterned, aminated surface; and (3) a specific interaction between the aminated surface and biomolecules (i.e., enzymes and proteins) and therefore a potential

* Author to whom correspondence should be addressed: fax +86-10-64416338; e-mail yangwt@mail.buct.edu.cn.

[†] State Key Laboratory of Chemical Resource Engineering and Department of Polymer Science, Beijing University of Chemical Technology.

[‡] College of Life Science and Technology, Beijing University of Chemical Technology.

10.1021/bm0605356 CCC: $33.50
Published on Web 09/23/2006

in biochips. As a continuation to the mass loss phenomenon of the PET substrate described in the former paper,[21] the present work mainly reports an effective patterned etching approach in order to fabricate micro/nanoscale wells and channels on PET with the use of photomasks, and a technique consisting of photochemical etching (USAR, step 1) and alkaline hydrolysis (step 2). The new aspects can be summarized as follows: (1) A regular well or channel did indeed remain after USAR and extraction. (2) The etching depth of the aminated region could be effectively deepened by a simple potassium hydroxide (KOH) wet treatment, while the etching on a blank (unaminated) region was not apparent by this treatment. (3) The etching depth could be further deepened by repeat photochemical (USAR) and wet (KOH) etchings. (4) We also found that step 1 gave an aminated surface and that step 2 could erase it. As a result, by repetitively performing steps 1 and 2, we could control not only the depth of the channels or wells but also functionalities on their inner surfaces. This was exemplified by the electrostatic self-assembly of an antibody (microarray) on such a surface in order to obtain bioassay functionalities. We expect that this facile fabrication method and the resulting micro/nanostructures with functionalized inner surfaces could provide potential platforms for microchips toward various functions such as microarrays, heterogeneous immunoassays, biosensors, concentrations, filtrations, and microanalysis.

Experimental Section

Materials and Reagents. A commercial PET film (100 μm in thickness) was cut into square samples with typical dimensions of 25 cm^2 (5 $\times$ 5 cm^2), which were then subjected to Soxhlet extraction with acetone for 24 h to remove impurities and additives before use. DMF (AR grade) and potassium hydroxide (KOH) (AR grade) were purchased from Beijing Chemical Reagents Co. and used without purification. Fluorescein isothiocyanate-labeled immunoglobulin (FITC−IgG) was obtained from Beijing Xin Jing Ke Biotechnology Co. Ltd, and stored at −15 °C before use.

Microfabrication Procedures. The step by step process can be described as follows:

Step 1. A predetermined amount of DMF was deposited on the bottom PET film with a microsyringe. A top BOPP (biaxially orientated polypropylene) film covered this solution and the drop of solution was spread into an even and very thin liquid layer under suitable pressure from a quartz plate. A metallic photomask was placed onto the BOPP film surface to control the irradiation area. This assembly was placed on the holder and irradiated from the top by UV light at room temperature (by a high-pressure mercury lamp, 1000 W). The UV intensity could be regulated by changing the distance between the sample and the lamp. After the irradiation, the bottom PET film was washed three times with copious amounts of acetone and subjected to Soxhlet extraction with acetone for 8 h, followed by three additional washings with acetone. Finally it was dried to constant weight.

Step 2. The film obtained from step 1 was soaked in an aqueous KOH solution (1 wt %) at 50 °C for a given time, taken out, and washed three times with copious amounts of deionized water. It was then dried at 50 °C to constant weight.

Ultrastep. The PET film after photoirradiation was taken out without Soxhlet extraction, washed three times with acetone, and soaked in a KOH solution in order to perform step 2.

Protein Immobilization. Detailed procedures have been referred to in a recent study.[21] The channel fabricated in step 1 was first protonated by soaking the structure in an acid solution with pH 2.0 for 30 min. Electrostatic self-assembly of IgG was achieved by incubating the protonated structure in a FITC−IgG/Tris-HCl solution (pH 7.8) for 30 min at 37 °C. Thorough washing with a buffer solution of Tris-HCl (pH 7.8) was performed to remove the nonspecific adsorption. A parallel experiment was conducted on the channel fabricated according to steps 1 and 2 or the ultrastep, followed by FITC−IgG assembly.

Characterization. X-ray photoelectron spectra (XPS) on the aminated surfaces were obtained by using a PHI-5300/XPS instrument (Al/Mg excitation, 45°). Fluorescent microscopic images were taken by a Nikon Eclipse E600W (λ_{ex} = 488 nm). Optical microscopic observations were carried out on a Nikon TE2000-s system (Tokyo, Japan). Scanning electron microscopy (SEM) was performed with a S250HK3 (Cambridge, U.K.) instrument. Atomic force microscopy (AFM) in tapping mode was carried out on a NanoScope IIIa (Digital Instruments Co., Santa Barbara, CA) instrument. Depth data of the wells and channels was obtained by section analysis in the software provided by the manufacturer (Digital Instruments Co., Santa Barbara, CA).

Results and Discussion

Figure 1A describes the fabrication procedure of a microwell. A thin DMF layer was sandwiched between films of PP and PET, and a photomask with a circular hole array pattern (photomask a in left image of Figure 1B) was placed onto the sandwich setup (a). A unique character assigned to this sandwich setup was its ability to distribute the reaction solution evenly on the polymer surface with a micrometer thickness. The reaction solution and polymer surface could then come into intimate contact as a result of the sandwiching pressure. This character has been demonstrated and used to develop several highly effective polymer surface modification techniques in our group.[21−23] In the present work, DMF reacted with ester groups along the PET chain on the UV-irradiated region to initiate an aminolysis reaction, resulting in the degradation of the PET chains.[21] After the irradiation, as well as Soxhlet extraction (8 h) with acetone to remove these degraded short chains, the etched well was formed (b) (step 1), and its depth could be tuned from 125 to 350 nm by controlling the irradiation time and the UV intensity (see below). The second step (step 2) was to use an aqueous KOH solution (1 wt %) at 50 °C to develop the formed structure, increasing the depths to 250−1400 nm (c). For fast prototyping, the irradiated surface without Soxhlet extraction could be directly exposed in the KOH solution to finish developing (ultrastep). The resulting structure had the same etching depth and shape as those in the two-step etching, with the prototyping time being shortened to 3−5 h. The cross-sectional shape of the final structure scanned by AFM was trapezoidal with smooth corners (middle image in Figure 1B). The width of the top of the well was measured to about 43 μm, by using the section analysis function from AFM (right image in Figure 1B). It was thus close to the size of photomask a (40 μm). The reason that the asymmetrical developing in KOH was successful was that the topography on the irradiated region became very rough after step 1 (Figure 2). This roughness facilitated the contact and the downward infiltration of KOH to the bottom of the structure, thereby increasing the alkaline hydrolysis rate.[24]

The etching depth could be controlled and conveniently tuned by the reaction conditions. When the photoirradiation time was increased in step 1, both the etching depths in steps 1 and 2 increased. For instance, the etching depths after step 2 at irradiation times of 4, 12, and 16 min were 250 nm, 800 nm, and 1.4 μm, respectively (Figure 3). Enhancement of the UV intensity in step 1 was also found to increase the etching depth (Figure 4). When the UV intensity changed from 9.5 mW/cm^2 (dashed line) to 18.5 mW/cm^2 (solid line), the etching depths at both steps 1 and 2 increased. The maximum etching depth, that is, 1.45 μm, was obtained at 18.5 mW/cm^2 after step 2.

Steps 1 and 2 were considered as a single-cycle total etching. Logically, a multiple-cycle total etching should be able to

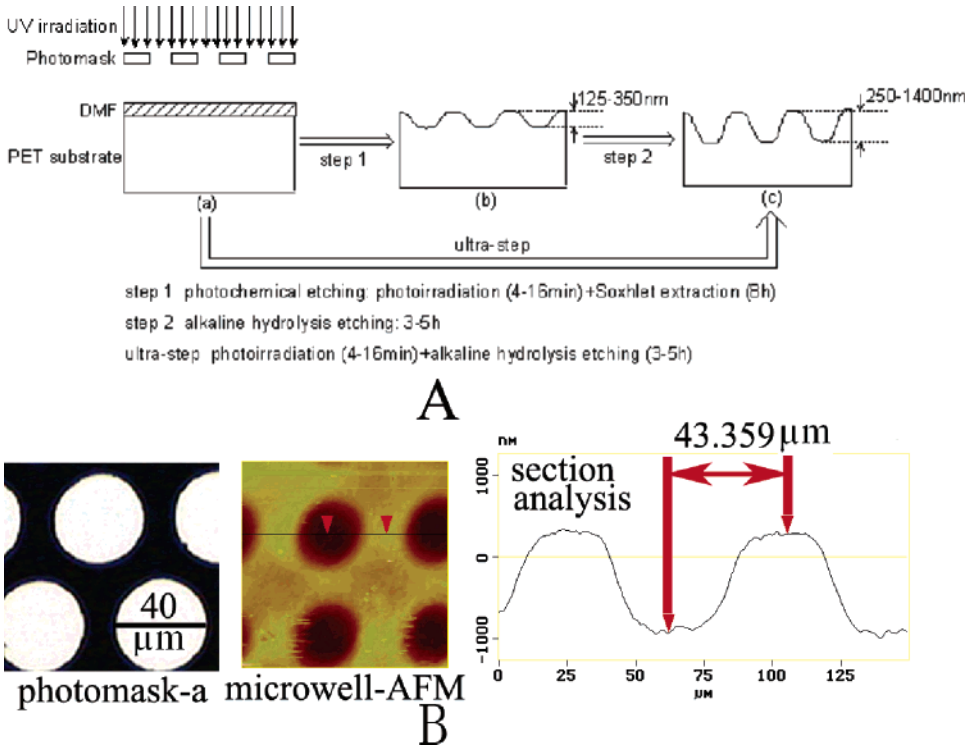

Figure 1. Stepwise chemical etching on a PET surface. (A) Schematic etching process; (B) surface and profile analysis of the microfabricated well.

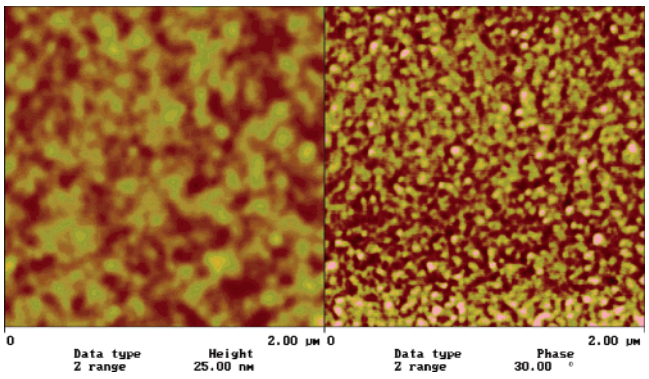

Figure 2. AFM image of an aminated surface after step 2 (left, height image; right, phase image).

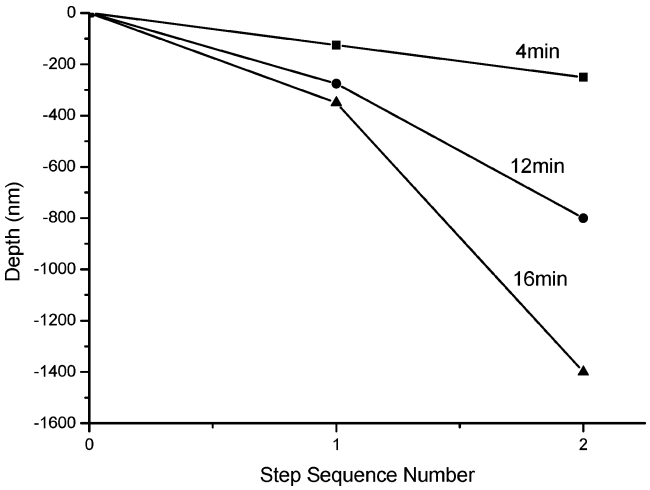

Figure 3. Effect of etching step and irradiation time on etching depth. The UV intensity is 18.5 mW/cm^2.

increase the etching depth further. To investigate this hypothesis, a photomask with a striped pattern (photomask b in Figure 7A) was used to fabricate microchannels through a single-cycle total etching. Subsequently, by means of a microscope, photomask b was placed on the same precise position on the substrate surface as during the first etching. The same procedure, that is, photochemical etching followed by alkaline hydrolysis, was conducted to obtain a second total etching. After a series of three such etching procedures, the etching depth increased linearly from the initial 1 μm to 6 μm, with the average etching depth each time being about 1.8 μm (Figure 5). Figure 1B proved that there was no obvious widening effect on the lateral size as a result of the single-cycle total etching. SEM images (top view) showed that the average microchannel width after a double-cycle total etching was 50 μm (inset b in Figure 5). The width thus approached the designed feature of photomask b (50 μm wide in region I of Figure 7A). However, further cross-sectional SEM images of these microchannels (inset c in Figure 5) showed an obvious widening effect of the tops of the channels. The widths were close to 100 μm and thus nearly 2 times the designed feature (50 μm). Fortunately, the top width of the channels after three total etching cycles was maintained at 100 μm (picture not shown), indicating that the side etching did not increase further after two cycles. This side etching is attributed to the isotropic developing from KOH, and a protection procedure to suppress this effect is needed.

With our method, it was possible to fabricate various micro/nanostructures, even structures with complex patterns (vide infra), simply by using a photomask with the desired pattern. However, a controlled functionalization of the inner surface of the structure was often required due to the demands from immunoaffinity chromatography,[25] heterogeneous immunoassays,[26] researching the cell activity,[27] immobilization of enzymes,[28] and carbohydrate analysis.[29] We have found that the aminolysis reaction in step 1 could incorporate tertiary

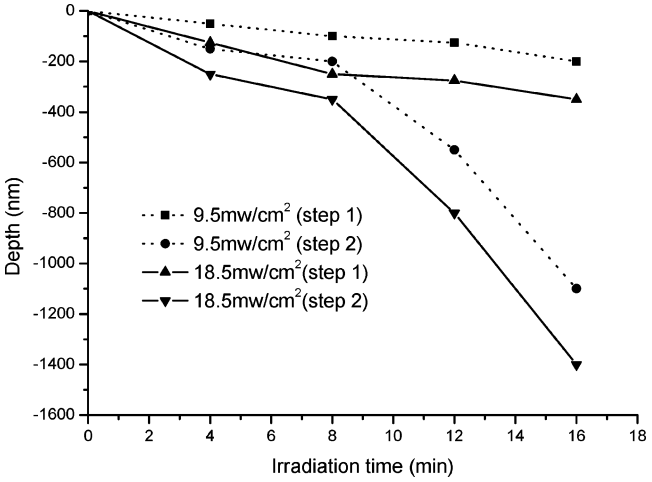

Figure 4. Effect of UV intensity on etching depth.

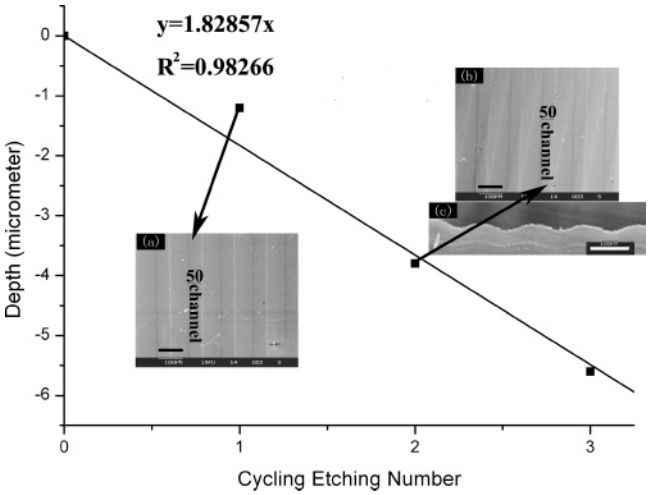

Figure 5. Effect of the number of etching cycles on etching depth. (Insets) Topographical SEM images of the microchannels after (a) single and (b) double total etching cycle. A cross-sectional SEM image of the microchannels after a double total etching cycle is shown in inset c. The bars in −the insets are 100 μm.

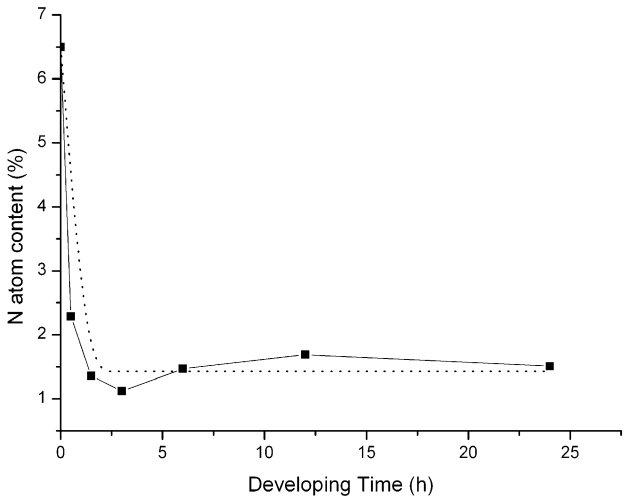

Figure 6. Effect of KOH developing time on the remaining nitrogen content of the etched surface. (—) Experimental data; (---) fitting curve for these data.

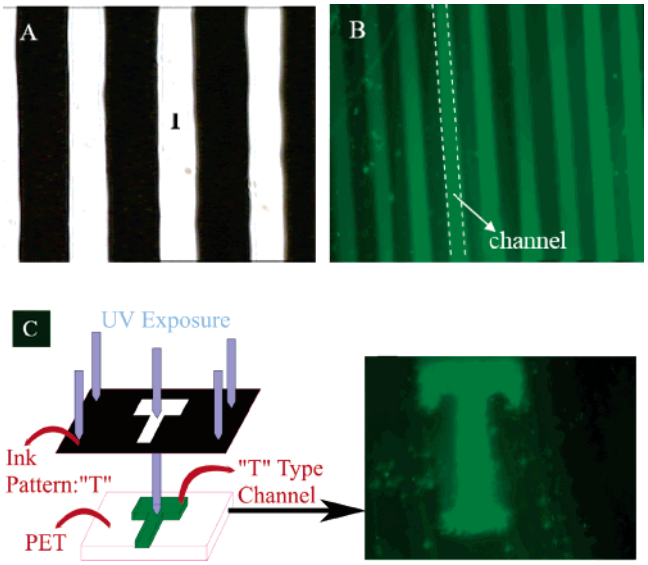

Figure 7. (A) Optical image of photomask b (region I represents a UV penetration void with a width of 50 μm). (B) Fluorescent image of the straight microchannel after step 1 and incubation in FITC−IgG solution for a given time. (C) Schematic etching process of a "T"-type microchannel (left picture) and the corresponding practical fluorescent image after incubation of the structure in a FITC−IgG solution for a given time (right image).

amines onto the irradiated region and have demonstrated that an effective microarray of FITC−IgG could be achieved on the patterned aminated surface through electrostatic interaction, with the signal-to-background ratio reaching about 5:1.[21] In fact, in the present work, the nitrogen content after step 1 was detected as 6.5%. The KOH developing for 2.5 h in step 2 decreased this content to about 1.5% (Figure 6), due to the dissociation and solution of the nitrogen-containing chains during the alkaline hydrolysis reaction. The nitrogen remained at this level as the developing time increased. This suggested that the developing process was terminated and became stable after 3 h, as shown by a fitting curve for the experimental data (dashed line in Figure 6).

The above-mentioned features showed that the flexibility in design of the pattern as well as functionalization of the inner surface provided us with a very simple approach for directly constructing various micro/nanodevices toward desired functions. For instance, by using photomask b (Figure 7A) and step 1, microchannels (1.4 μm in depth) were fabricated, showing a special affinity for antibodies. Under fluorescent microscopy, the microchannels (after incubation in the FITC−IgG solution) showed an ordered green stripe pattern with the width close to the feature of photomask b (Figure 7B). This demonstrated the successful incorporation of FITC−IgG (which is a green fluorescence protein) on the inner surface of the channel. Moreover, a "T"-type complex channel, another typical element in microfluidic chips, was fabricated on a PET surface (1.5 μm in depth). This was carried out by using a self-made ink T pattern printed on plastic film (left image in Figure 7C).[30] Such T-type channels fabricated by step 1 showed a similar affinity to FITC−IgG (right image in Figure 7C). In Figure 7B,C, the fluorescence signal from the PET background mainly came from the autofluorescence of this plastic.[21] This phenomenon was further demonstrated and investigated systematically in a recent publication.[31]

The great advantage of the present method was the possibility of controlling the phototriggered etching simply by use of a

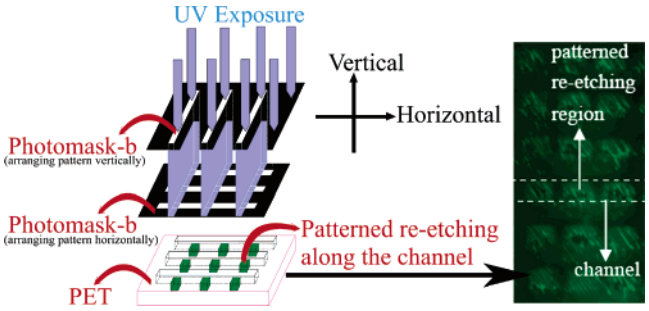

Figure 8. Schematic etching process of a patterned functionalization along the microchannel (left picture) and the corresponding practical fluorescent image after incubation of the structure in FITC−IgG solution for a given time (right image).

photomask. This allowed for an accurate modification of any channel region with micrometer resolution. This patterned modification along the inner surface of the channel plays a key role in heterogeneous immunoassays, biosensors, and microanalytical systems.[32] As described in Figure 8 (left image), photomask b was placed to exactly cover the channels (fabricated by the same photomask b and a two-step etching). Subsequently another mask of the same type as photomask b was applied perpendicularly onto the existing mask, giving rise to a crossed mask pattern. Such a setup was found to create a patterned re-etching along the existing channel bottoms through step 1, onto which the microarray of the antibody (FITC−IgG) was achieved. This was revealed by rectangular green regions along each channel (right image in Figure 8). In contrast, after step 2, the nitrogen content on the surface was largely diminished, and it was found that such a channel showed a slightly lower affinity for FITC−IgG compared with blank PET (picture not shown).

Summary and Conclusions

In conclusion, we have developed a novel combination etching method to fabricate shallow profiled micro/nanostructures on PET surfaces with short prototyping time (3−5 h). The amine functionality on the surface could be regulated by performing various etching steps: the resulting structure after step 1 had a high amine group content, which could be erased to a large extent by step 2. The present fabrication technique is low-cost and fast, which is expected to stimulate the development of large-scale applications of microchips toward various functions. One example to prove the potential application of this method was given through antibody adsorption and further patterning on the inner surface of channels fabricated by step 1.

Acknowledgment. We acknowledge funding of the Major Project (50433040) from National Natural Science Foundation of China (NSFC) and of the Major Project (XK100100433 and XK100100540) for Polymer Chemistry and Physics Subject Construction from Beijing Municipal Education Commission (BMEC).

References and Notes

(1) (a) Lynch, M.; Mosher, C.; Huff, J.; Nettikadan, S.; Johnson, J.; Henderson, E. *Proteomics* **2004**, *4*, 1695−1702. (b) Senaratne, W.; Andruzzi, L.; Ober, C. K. *Biomacromolecules* **2005**, *6*, 2427−2448. (c) Iwata, R.; Suk-In, P.; Hoven, V. P.; Takahara, A.; Akiyoshi, K.; Iwasaki, Y. *Biomacromolecules* **2004**, *5*, 2308−2314. (d) Ross, E. E.; Joubert, J. R.; Wysocki, R. J., Jr.; Nebesny, K.; Spratt, T.; O'Brien, D. F.; Saavedra, S. S. *Biomacromolecules* **2006**, *7*, 1393−1398.
(2) Stone, H. A.; Kim, S. *AICHE J.* **2001**, *47*, 1250−1254.
(3) Watts, P.; Haswell, S. J. *Chem. Eng. Technol.* **2005**, *28*, 290−301.
(4) Espina, V.; Mehta, A. I.; Winters, M. E.; Calvert, V.; Wulfkuhle, J.; Petricoin, E. F., III; Liotta, L. A. *Proteomics* **2003**, *3*, 2091−2100.
(5) Vikner, T.; Janasek, D.; Manz, A. *Anal. Chem.* **2004**, *76*, 3373−3386.
(6) Chow, A. W. *AICHE J.* **2002**, *48*, 1590−1595.
(7) (a) Felton, M. J. *Anal. Chem.* **2003**, *75*, 505A−508A. (b) Wu, Z.; Xanthopoulos, N.; Reymond, F.; Rossier, J. S.; Girault, H. H. *Electrophoresis* **2002**, *23*, 782−790.
(8) Park, M. B. C.; Yan, Y.; Neo, W. K.; Zhou, W.; Zhang, J.; Yue, C. Y. *Langmuir* **2003**, *19*, 4371−4380.
(9) (a) Cui, H.; Horiuchi, K.; Dutta, P.; Ivory, C. F. *Anal. Chem.* **2005**, *77*, 1303−1309. (b) Akin, D.; Li, H.; Bashir, R. *Nano Lett.* **2004**, *4*, 257−259. (c) Bouse, L.; Mouradian, S.; Minalla, A.; Yee, H.; Williams, K.; Dubrow, R. *Anal. Chem.* **2001**, *73*, 1207−1212.(d) Foote, R. S.; Khandurina, J.; Jacobson, S. C.; Ramsey, J. M. *Anal. Chem.* **2005**, *77*, 57−63. (e) Fu, A. Y.; Chou, H. P.; Spence, C.; Arnold, F. H.; Quake, S. R. *Anal. Chem.* **2002**, *74*, 2451−2457. (f) Dittrich, P. S.; Schwille, P. *Anal. Chem.* **2003**, *75*, 5767−5774.
(10) Sivanesan, P.; Okamoto, K.; English, D.; Lee, C. S.; Devoe, D. L. *Anal. Chem.* **2005**, *77*, 2252−2258.
(11) Ivanova, E. P.; Wright, J. P.; Pham, D.; Filipponi, L.; Viezzoli, A.; Nicolau, D. V. *Langmuir* **2002**, *18*, 9539−9546.
(12) (a) Zhu, H.; Klemic, J. F.; Chang, S.; Bertone, P.; Casamayor, A.; Klemic, K. G.; Smith, D.; Gerstein, M.; Read, M. A.; Snyder, M. *Nat. Genet.* **2000**, *26*, 283−289. (b) McDonald, J. C.; Metallo, S. J.; Whitesides, G. M. *Anal. Chem.* **2001**, *73*, 5645−5650.
(13) (a) Bernhard, D. D.; Mall, S.; Pantano, P. *Anal. Chem.* **2001**, *73*, 2484−2490. (b) Biran, I.; Walt, D. R. *Anal. Chem.* **2002**, *74*, 3046−3054. (c) Melechko, A. V.; Mcknight, T. E.; Guillorn, M. A.; Merkulor, V. I.; Ilic, B.; Doktycz, M. J.; Lowndes, D. H.; Simpson, M. L. *Appl. Phys. Lett.* **2003**, *82*, 976−978. (d) Czaplewski, D. A.; Kameoka, J.; Mathers, R.; Coates, G. W.; Craighead, H. G. *Appl. Phys. Lett.* **2003**, *83*, 4836−4838.
(14) (a) Hibara, A.; Saito, T.; Kim, H. B.; Tokeshi, M.; Ooi, T.; Nakan, M.; Kitamori, T. *Anal. Chem.* **2002**, *74*, 6170−6176. (b) Han, J.; Craighead, H. G. *Science* **2000**, *288*, 1026−1029. (c) Ionescu, R. E.; Marks, R. S.; Gheber, L. A. *Nano Lett.* **2003**, *3*, 1639.
(15) Yu, T.; Ober, C. K. *Biomacromolecules* **2003**, *4*, 1126−1131.
(16) Studer, V.; Pepin, A.; Chen, Y. *Appl. Phys. Lett.* **2002**, *80*, 3614−3616.
(17) (a) Guo, L. J.; Cheng, X.; Chou, C. F. *Nano Lett.* **2004**, *4*, 69−73. (b) Cao, H.; Yu, Z.; Wang, J.; Tegenfeldt, J. O.; Anstin, R. H.; Chen, F.; Wu, W.; Chou, S. Y. *Appl. Phys. Lett.* **2002**, *81*, 174−176.
(18) (a) Geissler, M.; Xia, Y. *Adv. Mater.* **2004**, *16*, 1249−1269. (b) Segalman, R. A. *Mater. Sci. Eng. R* **2005**, *48*, 191−226. (c) Park, M.; Harrison, C.; Chaikin, P. M.; Register, R. A.; Adamson, D. H.; et al. *Science* **1997**, *276*, 1401−1404. (d) Finne, A.; Andronova, N.; Albertsson, A.-C. *Biomacromolecules* **2003**, *4*, 1451−1456.
(19) Sivanesan, P.; Okamoto, K.; English, D.; Lee, C. S.; Devoe, D. L. *Anal. Chem.* **2005**, *77*, 2252−2258.
(20) Karlsson, A.; Karlsson, M.; Karlsson, R.; Sott, K.; Lundquist, A.; Tokarz, M.; Orwar, O. *Anal. Chem.* **2003**, *75*, 2529−2537.
(21) Yang, P.; Zhang, X.; Yang, B.; Zhao, H.; Chen, J.; Yang, W. *Adv. Funct. Mater.* **2005**, *15*, 1415−1425.
(22) Yang, P.; Deng, J.; Yang, W. *Macromol. Chem. Phys.* **2004**, *205*, 1096−1102.
(23) (a) Yang, P.; Deng, J.; Yang, W. *Polymer* **2003**, *44*, 7157−7164. (b) Yang, P.; Sun, Y.; Deng, J.; Liu, W.; Zhang, L.; Yang, W. *J. Polym. Sci. Part A: Polym. Chem.* **2004**, *42*, 4074−4083. (c) Yang, P.; Xie, J.; Yang, W. *Macromol. Rapid. Commun.* **2006**, *27*, 418−423.
(24) Sammon, C.; Yarwood, J.; Everall, N. *Polym. Degrad. Stabil.* **2000**, *67*, 149−158.
(25) Doherty, E. A. S.; Meagher, R. J.; Albarghouthi, M. N.; Barron, A. E. *Electrophoresis* **2003**, *24*, 34−54.
(26) (a) Yang, T.; Jung, S.; Mao, H.; Cremer, P. S. *Anal. Chem.* **2001**, *73*, 165−169. (b) Morier, P.; Vollet, C.; Michel, P. E.; Reymond, F.; Rossier, J. S. *Electrophoresis* **2004**, *25*, 3761−3768. (c) Rossier, J. S.; Girault, H. H. *Lab Chip* **2001**, *1*, 153−157.
(27) Williams, V.; Kashanin, D.; Shvets, I. V.; Mitchell, S.; Volkov, Y.; Kelleher, D. *J. Assoc. Lab. Autom.* **2002**, *7*, 135−141.
(28) Wang, J. *Electrophoresis* **2002**, *23*, 713−718.
(29) Suzuki, S.; Honda, S. *Electrophoresis* **2003**, *24*, 3577−3582.
(30) "T" pattern was designed via computer and printed onto hydrophilically modified PP surface (*Polymer* **2003**, *44*, 7157−7164) through an office laser printer (1200 dpi). Similar work was also reported by Whitesides' group (*Adv. Mater.* **1996**, *8*, 917).

(31) Piruska, A.; Nikcevic, I. S.; Lee, H.; Ahn, C.; Heineman, W. R.; Limbacha, P. A.; Seliskar, C. J. *Lab Chip* **2005**, *5*, 1348−1354.
(32) (a) Qu, H.; Wang, H.; Huang, Y.; Zhong, W.; Lu, H.; Kong, J.; Yang, P.; Liu, B. *Anal. Chem.* **2004**, *76*, 6426−6433. (b) Linder, V.; Sia, S. K.; Whitesides, G. M. *Anal. Chem.* **2005**, *77*, 64−71. (c) Chován, T.; Guttman, A. *Trends Biotechnol.* **2002**, *20*, 116−122. (d) Wang, Y.; Vaidya, B.; Farquar, H. D.; Stryjewski, W.; Hammer, R. P.; McCarley, R. L.; Soper, S. A.; Cheng, Y.-W.; Barany, F. *Anal. Chem.* **2003**, *75*, 1130−1140. (e) Dusseiller, M. R.; Niederberger, B.; Städler, B.; Falconnet, D.; Textor, M.; Vörös, J. *Lab Chip* **2005**, *5*, 1387−1392.

BM0605356